

# Using a Phantom to Compare MR Techniques for Determining the Ratio of Intraabdominal to Subcutaneous Adipose Tissue

Lane F. Donnelly<sup>1,2</sup>  
Kendall J. O'Brien<sup>1</sup>  
Bernard J. Dardzinski<sup>1,2</sup>  
Stacy A. Poe<sup>2</sup>  
Judy A. Bean<sup>2</sup>  
Scott K. Holland<sup>1,2</sup>  
Stephen R. Daniels<sup>2</sup>

**OBJECTIVE.** Patients who have a greater distribution of intraabdominal adipose tissue as compared with subcutaneous adipose tissue and an increased ratio of intraabdominal adipose tissue to subcutaneous adipose tissue are at greater risk for developing cardiovascular disease and type 2 diabetes mellitus. In previous MR investigations, researchers have used conventional T1-weighted spin-echo images to determine the ratio of intraabdominal adipose tissue to subcutaneous adipose tissue. However, no investigation, to our knowledge, has been performed to determine the accuracy of using different MR sequences to estimate adipose distribution. The purpose of our investigation was to compare MR imaging and segmentation techniques in calculating the ratio of intraabdominal to subcutaneous adipose tissue using an adiposity phantom.

**MATERIALS AND METHODS.** A phantom was created to simulate the distribution of subcutaneous and intraabdominal fat (with known volumes). Axial MR images were obtained twice through the phantom using a 5-mm slice thickness and zero gap for the following T1-weighted sequences: spin-echo, fast Dixon, and three-dimensional (3D) spoiled gradient-echo. An in-house computer software program was then used to segment the volumes of fat and calculate the volume of intraabdominal adipose tissue and subcutaneous adipose tissue and the ratio of intraabdominal to subcutaneous adipose tissue. Each imaging data set was segmented three times, so six sets of data were yielded for each imaging technique. The percentage predicted of the true volume was calculated for each MR imaging technique for each fat variable. The mean percentages for each variable were then compared using one-factor analysis of variance to determine whether differences exist among the three MR techniques.

**RESULTS.** The three MR imaging techniques had statistically significant different means for the predicted true volume of two variables: volume of subcutaneous adipose tissue ( $p < 0.001$ ) and volume of intraabdominal adipose tissue ( $p = 0.0426$ ). Estimates based on fast Dixon images were closest to the true volumes for all the variables. All MR imaging techniques performed similarly in estimating the ratio of intraabdominal adipose tissue to subcutaneous adipose tissue ( $p = 0.9117$ ). The acquisition time for the 3D spoiled gradient-echo images was 10–22 times faster than for the other sequences.

**CONCLUSION.** Conventional T1-weighted spin-echo MR imaging, the current sequence used in practice for measuring visceral adiposity, may not be the optimal MR sequence for this purpose. We found that the T1-weighted fast Dixon sequence was the most accurate at estimating all fat volumes. The T1-weighted 3D spoiled gradient-echo sequence generated similar ratios of intraabdominal to subcutaneous adipose tissue in a fraction of the acquisition time.

Received April 29, 2002; accepted after revision August 27, 2002.

<sup>1</sup>Department of Radiology, Cincinnati Children's Hospital Medical Center and University of Cincinnati, 3333 Burnet Ave., Cincinnati, OH 45229-3039. Address correspondence to L. F. Donnelly.

<sup>2</sup>Department of Pediatrics, Cincinnati Children's Hospital Medical Center and University of Cincinnati, Cincinnati, OH 45229-3039.

AJR 2003;180:993–998

0361–803X/03/1804–993

© American Roentgen Ray Society

**S**ubstantial evidence suggests that the distribution of adipose tissue in the abdomen and risk for cardiovascular disease and type 2 diabetes mellitus are related [1–5]. Patients with higher volumes of adipose tissue within the viscera (intraabdominal adipose tissue) than in the subcutaneous tissues surrounding the abdomen (subcutaneous adipose tissue) are at increased risk compared with patients who primarily

store fat in the subcutaneous adipose tissue [1–5]. Measurements of the ratio of intraabdominal adipose tissue to subcutaneous adipose tissue have been used on a research basis to estimate risk factors for cardiovascular disease and type 2 diabetes mellitus.

Currently, the most accurate way to predict the volume of fat in the intraabdominal adipose tissue and subcutaneous adipose tissue and calculate the ratio of intraabdominal

adipose tissue to subcutaneous adipose tissue is with cross-sectional imaging studies, such as CT or MR imaging [6–14]. Because it does not use ionizing radiation, MR imaging has been the modality of choice, particularly in longitudinal studies that require subjects to be imaged multiple times.

In previously published reports describing MR techniques used to calculate abdominal fat volumes and ratios, researchers have used conventional or fast T1-weighted spin-echo imaging to make these determinations [6–11]. However, other MR sequences may more accurately depict fat volumes than T1-weighted spin-echo sequences. In addition, there may also be MR techniques that can depict abdominal fat volumes as well as T1-weighted spin-echo sequences while having a shorter acquisition time. Because of the high cost related to magnet time for MR imaging, reducing acquisition time may prove important in minimizing costs when predicting fat volumes for either research or screening. The purpose of this study was to compare the accuracy of several MR imaging techniques in measuring abdominal fat distribution using an adiposity phantom.

## Materials and Methods

### Phantom

A phantom was created to simulate the distribution of subcutaneous and intraabdominal adipose tissues. The phantom was constructed of containers, IV fluid bags, and IV tubing filled with either water or dairy cream (38% fat by volume) (Fig. 1). Areas of water separated a central area containing fat (intraabdominal adipose tissue) from an external layer of fat (subcutaneous adipose tissue). The subcutaneous adipose tissue consisted of three

cream-filled fluid bags. The separating soft-tissue layer consisted of three water-filled fluid bags. The intraabdominal adipose tissue consisted of several cream-filled containers interspersed by several water-filled containers (as well as cream-filled IV tubing). The actual volumes of cream (i.e., fat) were 137 mL of intraabdominal adipose tissue and 690 mL of subcutaneous adipose tissue, for a total of 827 mL adipose tissue. The ratio of intraabdominal adipose tissue to subcutaneous adipose tissue was 0.199. The volume of fat in the tubing in the intraabdominal adipose tissue was 37 mL.

### Imaging Sequences

Three T1-weighted MR imaging sequences were evaluated for the ability to depict the volumes of fat in regions of the phantom. These sequences included conventional spin-echo images (Fig. 2A), fast Dixon images (Fig. 2B), and three-dimensional (3D) spoiled gradient-echo images (Fig. 2C). The spin-echo sequence was chosen because this sequence is the standard imaging technique of choice for studies investigating abdominal adiposity. The fast Dixon sequence was chosen because of its ability to generate images depicting fat signal only. The 3D spoiled gradient-echo sequence was chosen because of the short imaging time.

The phantom was placed in a transmit–receive head coil and imaged on a 1.5-T scanner (LX; General Electric Medical Systems, Milwaukee, WI). For each imaging sequence, images were obtained axially through the entire phantom. The following imaging parameters were constant for all three MR techniques: 5-mm slice thickness, zero gap, 24-cm field of view, and 1 excitation.

For the spin-echo images, the parameters were as follows: a TR/TE of 500/14, a  $256 \times 160$  matrix, and a total imaging time of 2 min 30 sec. For the 3D spoiled gradient-echo images, the parameters were 5.5/1.6, a  $60^\circ$  flip angle, a  $128 \times 128 \times 26$  matrix, and a total imaging time of 15 sec.

The fast Dixon images were created using a three-point Dixon technique that uses a fast spin-

echo sequence with a phase-correlation algorithm that provides online image reconstruction. Three images are generated per slice: one slice depicts pure water; one, pure fat; and another, combined fat and water [15–18]. For the fast Dixon images, imaging parameters included a TR of 500 msec and a TE of minimum full, a  $256 \times 160$  matrix, an echo-train length of 3, 6 slices per acquisition, 4 acquisitions, and a total imaging time of 5 min 30 sec. The fat-only data set was used to calculate the fat volumes.

Each T1-weighted MR imaging technique (conventional spin-echo, fast Dixon, and 3D spoiled gradient-echo) was performed two times.

### Data Segmentation to Determine Fat Volumes

The data obtained from the MR imaging sequences were transferred to a computer workstation. An in-house computer program (Cincinnati Children's Hospital Image Processing Software [CCHIPS/IDL]) written in Interactive Data Language (Research Systems, Boulder, CO) was used to segment the volumes of fat; calculate the total volume of adipose tissue, the volume of subcutaneous adipose tissue, and the volume of intraabdominal adipose tissue; determine the ratio of intraabdominal adipose tissue to subcutaneous adipose tissue; and measure the volume of fat in the tubing as a subregion of the intraabdominal adipose tissue.

The volume of fat for the different areas of the phantom was determined using all slices obtained through regions containing the phantom. The fraction of fat in a slice was determined in the following manner. Images were segmented into three different intensity levels (background, intermediate, and brightest) using a K-means clustering algorithm (Fig. 3). The volume of fat ( $\text{cm}^3$  or mL) for each slice was calculated by multiplying the area ( $\text{cm}^2$ ) of fat times 0.5 (5-mm slice thickness + 0-mm gap). The total volume of fat was then calculated by adding the volumes for the individual slices. The total volume of adipose tissue was calculated first, followed by the total volume of subcutaneous adipose tissue. The vol-

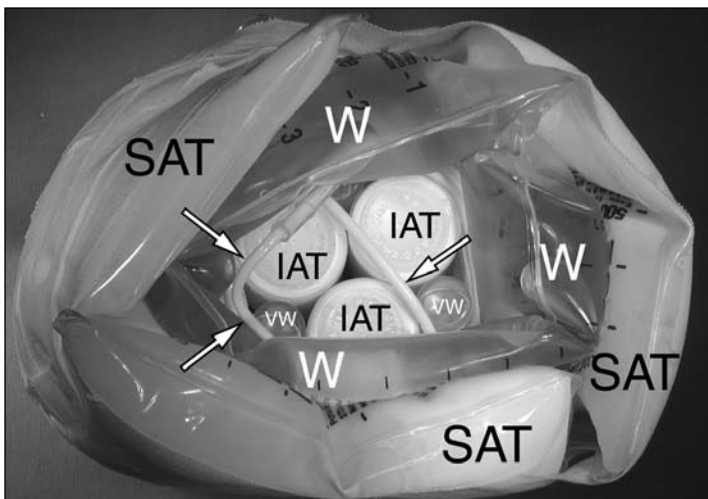


**Fig. 1.**—Photograph shows phantom used to simulate distribution of abdominal visceral and subcutaneous fat includes IV fluid bags, glass container, and IV tubing filled with either dairy creamer (to simulate fat) or water (to simulate soft tissues). Bags of water (W) separate external layer of fat (SAT), simulated by IV fluid bags full of cream, from central area of fat (IAT), simulated by containers and IV tubing (arrows) containing cream. Containers of water in central area (VW) simulate soft tissue interspersed between intraabdominal adipose tissue.

## Distribution of Adipose Tissue on MR Imaging

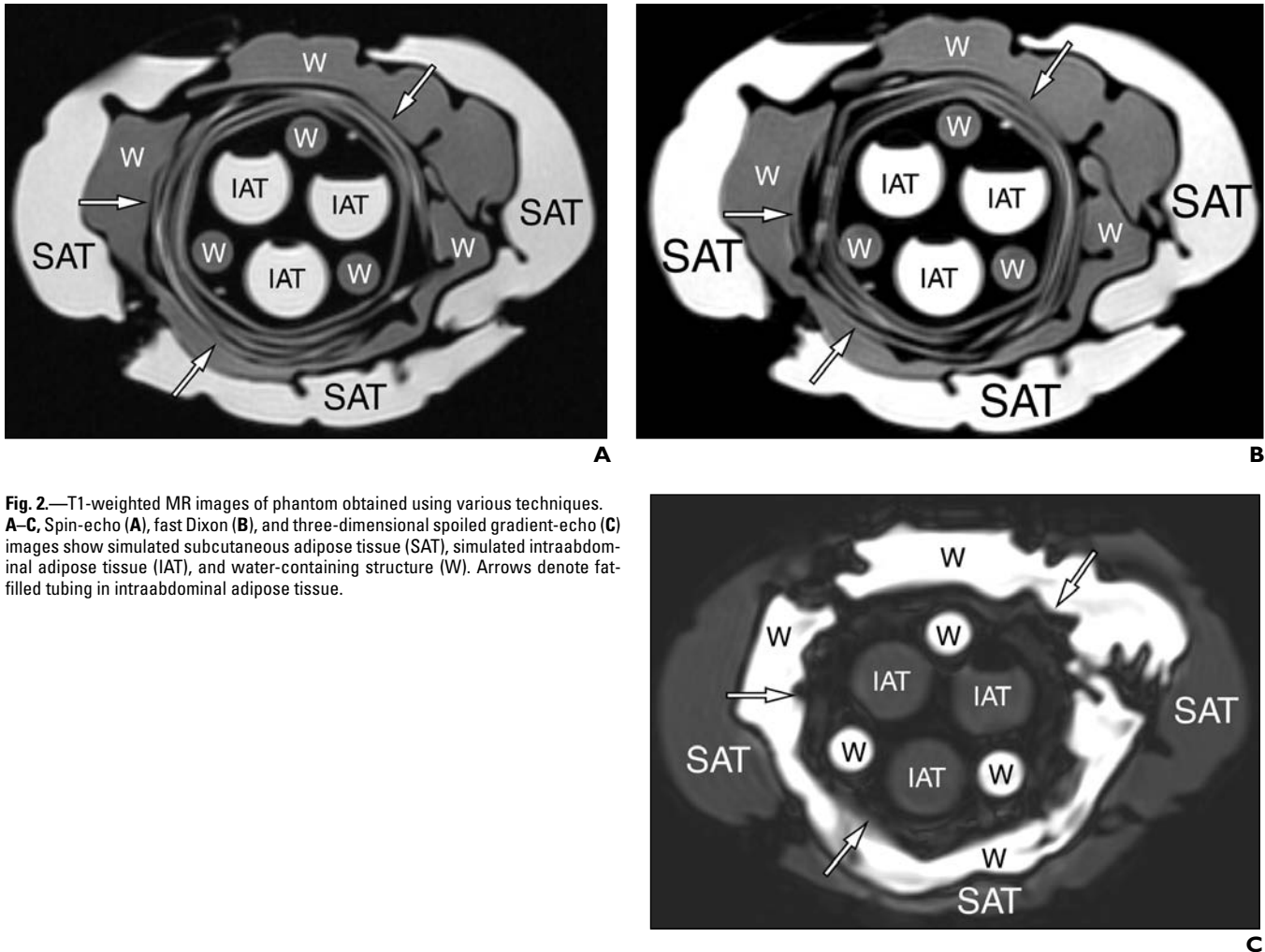


**Fig. 2.**—T1-weighted MR images of phantom obtained using various techniques. **A–C,** Spin-echo (**A**), fast Dixon (**B**), and three-dimensional spoiled gradient-echo (**C**) images show simulated subcutaneous adipose tissue (SAT), simulated intraabdominal adipose tissue (IAT), and water-containing structure (W). Arrows denote fat-filled tubing in intraabdominal adipose tissue.

ume of intraabdominal adipose tissue was then determined by subtracting the volume of subcutaneous adipose tissue from the total volume of adipose tissue. The estimated volume of fat in the tubing in the intraabdominal adipose tissue was also calculated.

Each of the two image sets from the MR sequences was segmented, and fat volumes were calculated on three separate occasions. Therefore, six data points were calculated for total volume of adipose tissue, volume of subcutaneous adipose tissue, volume of intraabdominal adipose tissue, ratio of intraabdominal to subcutaneous adipose tissue, and volume of fat in the tubing as a subregion of the intraabdominal adipose tissue for each imaging sequence (T1-weighted spin-echo, T1-weighted fast Dixon, and T1-weighted 3D spoiled gradient-echo).

### Statistical Analysis

For the six data sets, the mean values were calculated for the total volume of adipose tissue, the volume of intraabdominal adipose tissue, and the volume of subcutaneous adipose tissue; the ratio of intraabdominal adipose tissue to subcutaneous adi-

pose tissue; and the volume of fat in the tubing as a subregion of the intraabdominal adipose tissue. The percentage estimated of the true volume for each MR imaging technique for each parameter was then calculated by comparing the mean estimated fat volumes with the true known volumes in the phantom. A one-factor analysis of variance was then used to determine whether the ability of the three MR imaging techniques to predict the various fat volumes differed significantly. Bonferroni multiple comparison tests were used to determine individual differences among the MR imaging techniques. Statistical significance was defined as a *p* value of less than 0.05.

### Results

Table 1 summarizes the mean percentage of the estimated total volume, standard deviation, and statistical evaluations for volume of subcutaneous adipose tissue, volume of intraabdominal adipose tissue, and total volume of adipose tissue; the ratio of intraabdominal to subcutaneous adipose tissue; and

volume of fat in tubing as a subregion of intraabdominal adipose tissue. We detected statistically significant differences in the performance of the three imaging sequences for estimating all volumes of fat, but not for calculating the ratio of intraabdominal adipose tissue to subcutaneous adipose tissue.

The fat volume estimates based on the fast Dixon images were closest to the true volumes, whereas those based on the 3D spoiled gradient-echo images most poorly correlated with the true volumes. The percentage estimated of the true volume for the intraabdominal adipose tissue was lower than that for either the subcutaneous adipose tissue or total adipose tissue. This finding was related to the fact that the tubing containing fat was located in the intraabdominal adipose tissue. Because the tubing was smaller in caliber than the fluid bags of fat, all the imaging sequences were less accurate in detecting the volume of fat in

**TABLE I** Performance of Three MR Sequences to Estimate Volume and Ratio for Various Adipose Tissues

Adipose Tissue	T1-Weighted MR Imaging Technique	Estimate of True Volume (%)		p
		Mean	SD	
Subcutaneous volume	3D spoiled gradient-echo	80.53	4.87	<0.0001
	Fast Dixon	94.72	1.77	
	Spin-echo	86.50	2.30	
Intraabdominal volume	3D spoiled gradient-echo	58.70	10.75	0.0426
	Fast Dixon	69.70	3.94	
	Spin-echo	62.25	3.67	
Total volume	3D spoiled gradient-echo	76.90	5.42	<0.0001
	Fast Dixon	90.55	2.14	
	Spin-echo	82.48	2.54	
Ratio of intraabdominal to subcutaneous	3D spoiled gradient-echo	72.55	11.36	0.9117
	Fast Dixon	73.40	2.74	
	Spin-echo	71.68	2.44	
Intraabdominal volume in tubing	3D spoiled gradient-echo	0.00	0.00	<0.0001
	Fast Dixon	18.32	1.52	
	Spin-echo	1.27	1.18	

Note.—3D = three-dimensional.

the tubing. The mean percentage estimated of true volume of fat in the tubing was lower than that for either the subcutaneous adipose tissue or total adipose tissue. For the tubing alone, a statistically significant greater volume was estimated by the fast Dixon method than by the spin-echo and the 3D spoiled gradient-echo

imaging methods. The percentage predicted of true volume for the fat in the tubing alone was 18.32% for the fast Dixon sequence, 1.27% for the spin-echo sequence, and 0.00% for the 3D spoiled gradient-echo sequence.

Despite the statistically significant higher percentages estimated of true volume for all

the fat volumes by the fast Dixon method, all methods performed similarly in calculating the ratio of intraabdominal to subcutaneous adipose tissue. There was no statistically significant difference between any of the three sequences in estimating the percentage predicted of the true ratio. This finding suggests that all three sequences were consistently sensitive-insensitive in depicting the volumes of intraabdominal adipose tissue and subcutaneous adipose tissue.

**Discussion**

Subjects who store greater proportions of fat in the intraabdominal than in subcutaneous areas have been shown to be at an increased risk for cardiovascular disease and type 2 diabetes [1–14]. These patients have been shown to have a higher incidence of abnormalities of blood lipoprotein concentrations [1–14], higher triglyceride concentrations, higher circulating insulin levels, and higher incidence of hypertension [1–14]. Although the precise mechanism by which increased intraabdominal fat increases cardiovascular risk is unknown, researchers hypothesize that fat in the abdominal cavity is more metabolically active than that in the subcutaneous tissues. As obesity becomes an increasing health problem in the United States, a greater focus is being placed on investigations related to health risks associated with obesity.

A number of methods have been used in an attempt to accurately predict the ratio of intraabdominal adipose tissue to subcutaneous adipose tissue. Numerous studies have used the waist-hip circumference ratio or the thickness of a subcutaneous skin fold as a measure of fat distribution. However, only modest correlation has been found between the waist-hip ratio and amount of visceral fat measured using cross-sectional imaging [19, 20]. Individuals with the same body mass index and waist-hip ratio may have different amounts of fat deposited in the abdominal cavity [19, 20].

The most accurate methods currently available for measuring abdominal fat are CT [12–14] and MR imaging [6–11]. Both allow clear separation of adipose tissue from surrounding nonlipid tissue and the separation of intraabdominal from subcutaneous fat deposits. Other studies have shown that both methods are generally accurate in evaluating visceral adipose tissue [6–14]. The advantage of MR imaging is that it does not use ionizing radiation. This characteristic of MR imaging makes it more appropriate for longi-

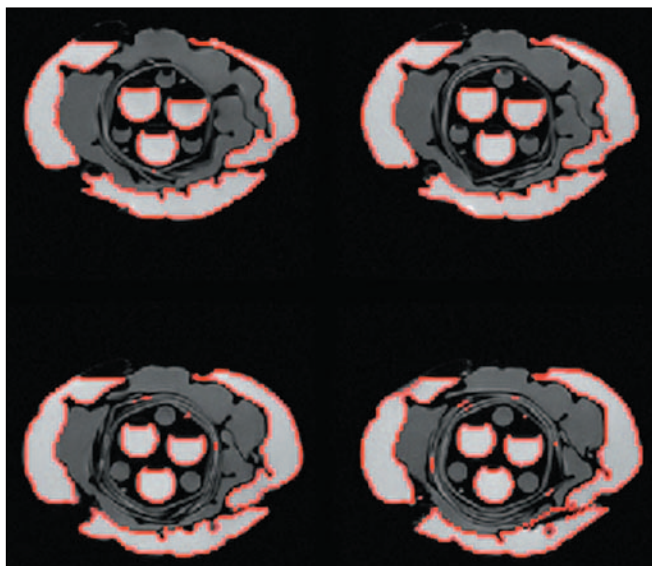


**Fig. 3.**—T1-weighted fast Dixon MR images of phantom reveal segmentation process. Signal equal to that of fat is identified. Note structures that contain signal equal to that of fat are outlined in red. Area of each region of interest can be calculated. Volumes can be calculated by adding areas of regions of interest from all axial slices containing area in question.

## Distribution of Adipose Tissue on MR Imaging

tudinal studies in which the cumulative dose of radiation may be a concern. In studies of women, the use of MR imaging also avoids exposing the ovaries to radiation.

Other researchers studying methods of estimating abdominal fat distribution have used MR imaging and T1-weighted spin-echo sequences [6–11]. T1-weighted spin-echo sequences are a reasonable choice for a number of reasons. This sequence is available on almost all MR scanners. Fat, unlike most other nonadipose tissues, appears high in signal intensity on T1-weighted images, so calculating the volume of fat with segmentation software is easy. However, little data, if any, have been published about whether alternative MR sequences may be more accurate in calculating fat volumes [6–11].

In our investigation, the fast Dixon technique was statistically more accurate in depicting fat than either the spin-echo technique or the 3D spoiled gradient-echo technique. In particular, the fast Dixon technique was statistically more accurate in depicting the volume of fat in smaller regions, simulated by the fat-filled tubing in the visceral adipose tissue of the phantom. Fast Dixon images revealed 18% of the fat in the smaller regions, compared with 1% depicted on spin-echo images and 0% on the 3D spoiled gradient-echo images ( $p < 0.0001$ ). Because adipose tissue in both the abdominal cavity and the subcutaneous tissues may be interspersed with nonadipose tissue, such as fascial planes, vascular structures, and enteric structures, the ability to depict small regions of fat may prove advantageous. Fast Dixon images are obtained using a spin-echo sequence with a phase-correction algorithm that produces three sets of images for each image slice: water, fat, and combined fat and water [15–18]. The images showing fat only create ideal data for estimating volumes through segmentation because no other tissues are shown.

Although accurate predictions of the volumes of fat in the intraabdominal and subcutaneous areas may be important for some studies, the variable most often used to study risk factors for cardiovascular disease and type 2 diabetes mellitus in most previous studies has been the ratio of intraabdominal adipose tissue to subcutaneous adipose tissue. In this study, all three MR techniques performed similarly in enabling this ratio to be estimated. Despite the statistically significant more accurate predictions of individual fat volumes based on images obtained with the fast Dixon technique, no statistically sig-

nificant difference was detected between the fast Dixon and the other imaging techniques in predicting the ratio of intraabdominal to subcutaneous adipose tissue. Even the 3D spoiled gradient-echo sequence, which performed poorly in estimating each of the individual volumes and detected none of the fat in the smaller regions, yielded a ratio of intraabdominal to subcutaneous adipose tissue that was similar to those yielded using the fast Dixon and T1-weighted sequences. Most likely related to consistent accuracy in depicting the intraabdominal adipose tissue and subcutaneous adipose tissue, the ratio of intraabdominal adipose tissue to subcutaneous adipose tissue may be accurately depicted by MR techniques that do not accurately depict the actual volumes of intraabdominal adipose tissue and subcutaneous adipose tissue.

Studies designed to screen a large number of subjects with MR imaging to predict only an intraabdominal to subcutaneous adipose tissue ratio may be more efficient using an MR sequence that can be performed rapidly, such as the 3D spoiled gradient-echo sequence. The acquisition time for the 3D spoiled gradient-echo sequence was 10 times shorter than that for the spin-echo sequence and 22 times faster than the fast Dixon sequence used in this study. These discrepancies in acquisition times may be important because one of the limiting factors in designing programs using MR imaging to quantify intraabdominal fat is the high expense of magnet time. Although the acquisition time is only a portion of the time that is required to scan a patient, a single rapid MR sequence would be ideal to increase patient throughput and compliance, reduce motion artifacts, and decrease cost.

The most cost-effective means by which to study intraabdominal adipose tissue remains to be determined. The accurate determination of intraabdominal adipose tissue is likely to be necessary for studies that focus on the mechanism of action of intraabdominal adipose tissue that produces an increase risk for cardiovascular disease. For these studies, the fast Dixon images are likely to provide the most accurate and useful information.

There are several limitations related to the information gained about the 3D spoiled gradient-echo sequence used in this study. The TE used for the 3D spoiled gradient-echo sequence in this series (1.6 msec) was chosen to minimize the time of series acquisition. The TE was not chosen to maximize the separation of fat and water tissues. Future studies may be

warranted to optimize the 3D spoiled gradient-echo sequence parameters for this specific task. Also, the standard deviation for the 3D spoiled gradient-echo sequence used in this series was four times greater than that used in other series, which may render the 3D spoiled gradient-echo sequences of limited value. This large standard deviation could result from the variation in signal intensity in our phantom because of large changes in magnetic susceptibility at the air–“tissue” interfaces.

In conclusion, conventional T1-weighted spin-echo images, the current MR sequence of practice for measuring visceral adiposity, may not be the optimal choice for this purpose. Of the MR imaging sequences tested, the fast Dixon technique, which segments data into fat and water data sets, was significantly most accurate for depicting volumes of fat. However, all the imaging sequences performed equally well in enabling the ratio of intraabdominal adipose tissue to subcutaneous adipose tissue to be estimated, suggesting that a rapid imaging sequence, such as 3D spoiled gradient-echo imaging, may be adequate for estimating this ratio. The acquisition time for the 3D spoiled gradient-echo sequence was 10–22 times faster than that of the other MR sequences.

## References

1. Blair D, Habicht J-P, Sims EAH, Sulwester D, Abraham S. Evidence for an increased risk for hypertension with centrally located body fat and the effect of race and sex on this risk. *Am J Epidemiol* **1984**;119:526–540
2. Nakajima T, Matsuzawa Y, Tokunaga K, Furioka S, Tarui S. Correlation of intra-abdominal fat accumulation and left ventricular performance of obesity. *Am J Cardiol* **1989**;64:369–373
3. Kissebah AH, Peiris AN, Evans DJ. Mechanisms associating body fat distribution to glucose intolerance and diabetes mellitus: window with a view. *Acta Med Scand* **1988**;723:79–90
4. Despres JP. The insulin resistance-dyslipidemic syndrome of visceral obesity: effect on patients' risk. *Obes Res* **1998**;6[suppl 1]:8S–17S
5. Kissebah AH. Central obesity: measurement and metabolic effects. *Diabetes Reviews* **1997**;5:8–20
6. Caprio S, Hyman LD, McCarthy S, Lange R, Bronson M, Tamborlane WV. Fat distribution and cardiovascular risk factors in obese adolescent girls: importance of the intraabdominal fat deposit. *Am J Clin Nutr* **1996**;64:12–17
7. Ross R, Rissanen J, Hudson R. Sensitivity associated with the identification of visceral adipose tissue levels using waist circumference in men and women: effects of weight loss. *Int J Obes Relat Metab Disord* **1996**;20:533–538
8. Owens S, Gutin B, Ferguson M, Allison J, Karp W, Le NA. Visceral adipose tissue and cardiovascular risk factors in obese children. *J Pediatr* **1998**;

- 133:41–45
9. Riches FM, Watts GF, Hua J, Stewart GR, Naoumova RP, Barrett PHR. Reduction in visceral adipose tissue is associated with improvement in apolipoprotein B-100 metabolism in obese men. *J Clin Endocrinol Metab* **1999**;84:2854–2861
  10. Chan YL, Leung SSF, Lam WWM, Peng XH, Metreweli C. Body fat estimation in children by magnetic resonance imaging, bioelectrical impedance, skinfold and body mass index: a pilot study. *J Paediatr Child Health* **1998**;34:22–28
  11. de Ridder CM, de Boer RW, Seidell JC, et al. Body fat distribution in pubertal girls quantified by magnetic resonance imaging. *Int J Obes* **1992**;16:443–449
  12. Goran MI, Gower BA. Relation between visceral fat and disease risk in children and adolescents. *Am J Clin Nutr* **1999**;70:149S–156S
  13. Goran MI, Nagy TR, Treuth MS, et al. Visceral fat in white and African American prepubertal children. *Am J Clin Nutr* **1997**;65:1703–1708
  14. Kvist H, Chowdhury B, Grangard U, Tuyen U, Sjostrom L. Total and visceral adipose-tissue volumes derived from measurements with computed tomography in adult men and women: predictive equations. *Am J Clin Nutr* **1988**;48:1351–1361
  15. Dixon WT. Simple proton spectroscopic imaging. *Radiology* **1984**;153:189–194
  16. Glover GH. Multipoint Dixon technique for water and fat proton and susceptibility imaging. *J Magn Reson Imaging* **1991**;1:521–530
  17. Glover GH, Schneider E. Three-point Dixon technique for true water/fat decomposition with B0 field inhomogeneity correction. *Magn Reson Med* **1991**;18:371–383
  18. Rybicki FJ, Chung T, Reid J, Jaramillo D, Mulkeren RV, Ma J. Fast three-point Dixon MR imaging using low-resolution images for phase correction: a comparison with chemical shift selective fat suppression for pediatric musculoskeletal imaging. *AJR* **2001**;177:1019–1023
  19. Despres JP, Prud'homme D, Pouliot M-C, Tremblay A, Bouchard C. Estimation of deep abdominal adipose-tissue accumulation from simple anthropometric measurements in men. *Am J Clin Nutr* **1991**;54:471–477
  20. van der Kooy K, Seidell JC. Techniques for the measurement of visceral fat: a practical guide. *Int J Obes* **1993**;17:187–196

The 2003 ARRS Annual Meeting Categorical Course will focus on oncologic imaging and will include sessions on CT, MR imaging, and FDG positron emission tomography.